ORIGINAL PAPER

Application of a new dithizone grafted polymeric adsorbent for solid phase microextraction of manganese and copper prior to FAAS in fortified vegetables and barbecue samples

Songül Ulusoy[1] · Ahmet Demirbaş[2] · Adil Elik[3] · Nail Altunay[3] · Gökhan Sarp[4] · Erkan Yılmaz[4] · Halil İbrahim Ulusoy[5]

Abstract

A new potential solid phase material called as dithizone@PAA was synthesized for first times, characterized and utilized as an easy versatile polymeric sorbent for the shake-assisted dispersive solid-phase micro-extraction of Mn(II) and Cu(II) ions from fortified vegetables and barbecue samples followed by flame atomic absorption spectrometry. The proposed approach is based on batch type solid phase extraction of Mn(II) and Cu(II) ions prior to their flame atomic absorption analysis (FAAS). All experimental variables were examined and optimized in detail. Using the optimized values, the dynamic linear range for Mn(II) and Cu(II) ions was 0.70–150.00 and 0.20–125.00 ng mL^{-1}, respectively, and the limits of detection for Mn(II) and Cu(II) ions were 0.20 and 0.06 ng mL^{-1}, respectively. The preconcentration factor was 50 for both analytes. The relative standard deviations of 3.1% and 2.5% were obtained at 75.00 ng mL^{-1} level of Mn(II) and Cu(II) ions. The precision and accuracy of the proposed method were investigated by the certified reference materials via intraday and inter-day studies. Finally, the results showed that the method was successfully applied for determining Mn (II) and Cu (II) ions in selected food samples with good recoveries.

Keywords Solid-phase microextraction · Flame atomic absorption spectrometry · Manganese · Copper · Fortified vegetables · Barbecue samples

Introduction

Today, the importance given to healthy food products is getting increased due to the increasing environmental problems (Walker et al. 2010). Since vegetables and meat products are rich in minerals, protein, fibers, and antioxidants, they undoubtedly have an important place in a healthy and balanced diet (Li and Komarek 2017). Due to chemical environmental pollution of toxic pollutants such as heavy metals, herbicides, pesticides, polyromantic hydrocarbons, and dioxins can be transmitted to vegetables and meat products in various ways (Carvalho, 2017). It is necessary to analyze the foodstuffs to ensure that the levels of these contaminants meet the agreed international requirements, taking into account the potential toxicity and consumption of vegetables and meat products (Ogunkunle et al. 2014). Trace levels of some metal ions such as manganese (Mn) and copper (Cu) have been reported to contribute to the prevention of some diseases caused by oxidative stress, as they have antioxidant and anti-mutagenic effects (Nimse and Pal 2015). However, these metal ions are toxic when exposed above certain levels. Therefore, the daily intake for Mn and Cu is limited to 2.0–5.0 mg day^{-1} and 1.2–1.6 mg day^{-1}, respectively (Tokman 2007). In this context, it is necessary and important to develop new, fast, and accessible analytical techniques for the determination of metal species at high toxic effects in food products.

✉ Nail Altunay
naltunay@cumhuriyet.edu.tr

1 Department of Pharmacy, Vocational School of Health Service, Cumhuriyet University, 58140 Sivas, Turkey

2 Department of Plant and Animal Production, Sivas Cumhuriyet University, Sivas, Turkey

3 Department of ChemistryFaculty of Science, Sivas Cumhuriyet University, Sivas, Turkey

4 Department of Analytical Chemistry, Faculty of Pharmacy, Erciyes University, Kayseri, Turkey

5 Department of Analytical Chemistry, Faculty of Pharmacy, Sivas Cumhuriyet University, Sivas, Turkey

Distinct analytical techniques including high-resolution inductively-coupled plasma mass spectrometry (HR-ICP-MS) (Rapp et al. 2017), inductively coupled plasma sector field mass spectrometry (ICP-SFMS) (Vassileva et al. 2019), inductively coupled plasma atomic emission spectrometry (ICP-AES) (Didukh et al. 2016), energy-dispersive X-ray fluorescence spectrometry (EDXRF) (Pytlakowska et al. 2018), graphite furnace atomic absorption spectrometry (GFAAS) (Manjusha et al. 2019), and flame atomic absorption spectrometry (FAAS) (Pourjavid et al. 2016) were developed for determination of manganese and copper in various food samples. Although techniques such as the HR-ICP-MS, ICP-SFMS, and ICP-AES have high selectivity, they have disadvantages such as operating costs and the requirement of highly qualified laboratory professionals (Gouda et al. 2020). On the other hand, the FAAS is widely used in metal analysis due to its speed, simplicity, inexpensive equipment requirements and wide application area for most kind of samples (Altunay et al. 2018).

In trace level analysis, matrix effect and low sensitivity of analytical techniques are two main problems for analyst. To overcome these problems, sample preparation methods such as magnetic solid phase microextraction (MSPME) (Meira et al. 2018), vortex-assisted dispersive liquid–liquid microextraction (VA-DLLME) (Elik et al. 2017; Ali et al. 2021), liquid–liquid microextraction procedure based on ionic liquid-assisted microemulsion (IL-µE-DLLME) (Arain et al. 2016), ultrasound-assisted dispersive-micro-solid phase extraction (US-D-µ-SPE) (Shirkhanloo et al. 2016), dual-cloud point extraction (d-CPE) (Peng et al. 2015), deep eutectic solvent-based ultrasound-assisted liquid phase microextraction (DES-UALPME) (Menghwar et al. 2019), magnetic solid phase microextraction (MSPME) (Acikkapi et al. 2019) and ultrasonic-assisted supramolecular solvent liquid–liquid microextraction (UA-Ss-LLME) (Altunay and Katin, 2020) have been frequently used for sensitive analysis of analytes. Conventional extraction methods are mainly focused on extraction of target ions via a chelating agent into an organic solvent. As well known, use of toxic organic solvents is not allowed in green chemistry approaches. So, solid phase extraction methods attract great attention with easy applicable and non-toxic properties. Especially, if re-usable materials can be developed, they can also be used a potential adsorbent in development of new devices for sensitive and practical analysis of trace species.

In the current study, it was explored an economical and green adsorbent based on the new synthesized dithizone@PAA for the preconcentration and separation of Mn(II) and Cu(II) in fortified vegetables and barbecue samples prior to the determination by FAAS. By the way, a useful adsorbent has been prepared by means of grafting dithizone molecule, which is a good chelating agent for Cu and Mn ions, to PAA structure as carrier. The characterization of the physicochemical properties of the adsorbent was evaluated by X-ray diffraction (XRD), Raman spectroscopy, Fourier transform infrared (FT-IR) spectroscopy and scanning electron microscopy (SEM). Relevant chemical parameters for the adsorption of Mn (II) and Cu(II) ions to the synthesized adsorbent were evaluated using computational chemistry methods. Adsorption and desorption parameters affecting the SA-DSPE including the effect of pH, adsorbent amount, adsorption time, eluent solvent type and volume, and desorption time were investigated in detail. The synthesized adsorbent exhibited good absorption properties for target ions. Before analyzing the selected samples, the developed method was validated by the analysis of certified reference materials in intraday and inter-day studies.

Experimental

Materials and chemicals

Mn(II) and Cu(II) nitrate salts were obtained from Merck (Darmstadt, Germany) and 1000 mg L^{-1} of stock solutions were prepared by using ultra-pure water. Working solutions were prepared by diluting the appropriate amount of stock solutions. Ethanol, tetrahydrofuran (THF), sodium hydroxide and nitric acid were supplied from Sigma (Sigma-Aldrich, St. Louis, MO, USA), while methanol, hydrochloric acid, and acetonitrile were supplied from Merck. The pH 4.0 of acetate buffer solution was prepared by adding 1.861 g of sodium acetate (Merck) and 4.643 g of acetic acid (Sigma) to a 100 mL flask. Deionized water (18.2 mΩ cm^{-1}) was obtained from a Milli-Direct Q3 purification system (Bedford, MA, USA). Certified reference materials including SRM-1568 Rice Flour, INCT-TL-1 Tea leaves, INCT-MPH-2 Mixed Polish Herbs and SRM-1515 apple leaves were used to assess the accuracy of the proposed method. Dithizone, N, N Bis-methylenebisacrylamide (Bis, AA) and N,N,N',N'-Tetramethyl-ethylenediamine (TEMED) were supplied from Sigma.

Apparatus

The quantification of Mn and Cu was achieved using an AA-6300 Shimadzu (Kyoto, Japan) FAAS equipped with a deuterium background corrector. The vortex VG3 model (IKA GmbH, Germany) was utilized for desorption step. The characterization of the adsorbent was evaluated by Fourier transform infrared spectroscopy (PerkinElmer Lambda 25), scanning electron microscopy (Zeiss Gemini 500) and energy-dispersive X-ray spectroscopy (Zeiss Gemini 500) techniques. Microwave equipment (Milestone Ethos, Italy) was used for the digestion of fortified vegetable samples and certified reference materials. Multi Bio RS-24 model

orbital rotator (BioSan, Berlin, Germany) and VG3 model vortex (IKA GmbH, Germany) were used for the adsorption and desorption steps, respectively. A digital pH-meter (Selecta 2001 Sartorius, North America) was used for pH measurement.

Preparation of fortified vegetable samples

In the study, soil taken from the research area of plant and animal production department from 0 to 30 cm depth was used. The soil was slightly alkaline (pH 7.88), low organic matter content (1.24%), sandy loam, calcareous (11.0%), low phosphorus concentration (426 kg ha^{-1}) and potassium concentration was sufficient (1151 kg ha^{-1}). 3-kg capacity plastic pot was used in the study, which was conducted in three replications according to the randomized plot trial pattern under greenhouse conditions. Sesame, peanut, eggplant, maize and cucumber plants were used as test plants. As basic fertilization, with planting, 100 mg N kg^{-1} for sesame, 200 mg N kg^{-1} for peanut, eggplant, corn and cucumber plants, 100 mg P kg^{-1}, 125 mg K kg^{-1}, 2.5 mg Fe kg^{-1} and 2.5 mg Zn kg^{-1} were applied for all plants. In the current preparation, manganese and copper doses were 0, 0.1 and 0.2 mg kg^{-1} and applied in the form of $MnSO_4 \cdot H_2O$ and $Cu(NO_3)_2 \cdot 3H_2O$, respectively. The plants were harvested 55 days after planting, and the above ground parts were washed in the laboratory with distilled water and dried at 70 °C for 48 h. Plants dried to constant weight were ground in an agate mill. By taking 0.2 g from the ground plants, a mixture of H_2O_2-HNO_3 (2 mL H_2O_2, 5 mL HNO_3) was added for digestion in a microwave system. The digestion step was performed for 3 min at 250 W, 5 min at 0 W, 5 min at 250 W, 3 min at 400 W, 10 min at 550 W, and then venting for 5 min.

Pre-treatment of barbecue samples

Five samples of meat doner, chicken doner, meatballs, grilled chicken and fish were used as application area of the proposed method. Samples were brought to the laboratory under cold chain at 4 °C and samples that would not be analyzed immediately were stored in the freezer − 20 °C. Microwave vessels (PTFE) were washed by 10 mL of concentrated HNO_3, heated for 15 min at 180 °C (800 W), and then rinsed with ultrapure water heated for 15 min at 180 °C before each digestion. All samples were accurately weighted as 0.50 g and transferred directly into microwave vessels, and 5 mL of concentrated HNO_3 was added. The blank solutions which contain 5 mL of concentrated HNO_3 were also prepared during the analysis of each sample. The digestion program was chosen in agreement with manufacturer's recommendations and published studies on microwave-assisted digestion optimization (Oymak et al. 2017).

Synthesis studies

New synthesized solid phase material (Dithizone@PAA) was easily prepared by using a simple procedure as explained in our previous studies (Ulusoy 2017; Şimşek et al. 2017; Şimşek and Ulusoy, 2016). Briefly, 2.0 g of acryl amide monomer and 0.25 g of cross-linker (Bis,AA) were homogeneously dissolved in 5 mL of ultra-pure water. Then, 300 mg of dithizone was added to this mixture during stirring on a magnetic stirrer. After a clear solution was obtained, 50 mg $(NH_4)_2S_2O_8$ was added as the initiator of polymerization reaction. Finally, the TEMED was added to solution to stabilize the polymers, while the system was getting cold by adding cold ultra-pure water. The synthesized polymer was washed with water for five times and ethanol for two times. Then, the obtained particles were dried for 24 h in a 50 °C vacuum oven and ground in a mortar and passed through a 1.2 mm sieve. The synthesized solid phase material was stored in the dark bottle.

Developed SA-DSPME procedure

The developed method consists of adsorption and desorption steps. For the adsorption step, 55 mg of Dithizone@PAA adsorbent was added to the centrifuge tubes containing 30 mL of sample solution including Mn(II) and Cu(II) ions in the optimized range). Then, the pH of the solution was adjusted to pH 4.0 with acetate buffer. In order to achieve adsorption of target ions on the adsorbent, the centrifuge tubes were placed on an orbital rotator and then shaken for 20 min. After centrifugation (4000 rpm, 2 min), the solid adsorbent containing analytes was collected at the bottom of tubes by centrifugation. The adsorption step was completed by discharging the aqueous part. Before the determination of analytes with FAAS, the analyte ions attached to the solid phase should be desorbed by using a suitable solvent. Therefore, 2.0 mL acidic ethanol was added to the adsorbents for the desorption step and vortexed for 80 s. At the end of this period, the solution after filtration was submitted to the nebulizer of FAAS, and of the contents of solution for Mn and Cu ions were determined by developed method. In order to minimize the errors that may occur from the reagents used, all steps described above were applied to the blank sample solution.

Results and discussion

Characterization assessment

FT-IR results

The FT-IR spectra obtained (see Fig. 1a) for Dithizone@PAA, Dithizone and Polyacrylamide (PAA) materials are in the wavelength range of 4000–450 cm^{-1}. The peaks of the Dithizone material were shown as characteristic peaks originating from the S–C=N and S–H functional groups at wavelengths of 1381.30 and 2044.1 cm^{-1}, respectively (Godwin-Uranta et al. 2018). In the 2970–2900 cm^{-1}wavelength range, the peaks observed at 2962.1 and 2909.9 cm^{-1} wavelengths are C–H symmetrical stretch-induced peaks, respectively. The sharp peak seen at 1590 cm^{-1} at ~ 1600 cm^{-1} wavelengths is thought to be a –C–N symmetrical stretching peak. The sharp peak with a wavelength of 1590 cm^{-1} at ~ 1600 cm^{-1} wavelength is thought to be a –C–N symmetrical stretching peak. Symmetrical stress peaks based on C–O and –C–O–C functional groups are observed at 1142.2 and 1212.2 cm^{-1} wavelengths, respectively. The 746.57 cm^{-1} peak seen in the fingerprint region is the –CH$_2$ asymmetric bending peak. It is seen that the peak seen at 675.58 cm^{-1} wavelength is an out-of-plane bending peak originating from –HC=CH-(cis) (Godwin-Uranta et al. 2018). The peak N–H with a wavelength of 3300 cm^{-1} seen in the wavelength range of 3300–3240 cm^{-1} of the PAA material is due to the secondary amine-based asymmetric stretching. The peak with a wavelength of 3182 cm^{-1} is the characteristic primary amine-based (NH$_2$) symmetrical stress peak. The peaks seen at 1601.4 and 1644.4 cm^{-1}, respectively, define the C–O–NH$_2$ and C=O stress peaks. 1408.2 and 1443.3 cm^{-1} peaks observed in the wavelength range of 1450–1400 cm^{-1} are seen as COO-symmetrical stress peaks (Chiem et al. 2006; Adhikary et al. 2007). After the synthesis, as can be seen in the spectrum of the final product (Dithizone@PAA), peaks in the wavelength range of 3300–3100 cm^{-1} originating from PAA were observed, and the Dithizone@PAA nanomaterial was successfully synthesized with the SH characteristic peak at 2044 cm^{-1} originating from dithizone. It has been proven by the obtained spectra that the peaks of Dithizone below 1500 cm^{-1} are suppressed by PAA.

Raman results

Raman spectra of Dithizone@PAA, PAA and Dithizone materials (see Fig. 1b) were obtained by using 532 nm laser as excitation source in Raman spectrophotometer. Due to the low interference in the Raman spectrum of the dithizone material, the detailed spectrum of dithizone is included. The main peaks of the Dithizone material are 602, 756, 854, 1229, 1243, 1375 and 1461 cm^{-1} wavelengths of Raman spectra, respectively. Raman spectrum with 1461 cm^{-1} wavelength in the 1410–1465 cm^{-1} wavelength range belongs to the energy bands formed as a result of the deformation of the –CH$_2$, –CH$_3$ functional groups. Considering the dithizone molecular structure, the 1375 cm^{-1} wavelength Raman spectrum is seen as the characteristic peak that performs the Umbrella mode oscillation (Saadati et al. 2020). Weak peaks at 1229 and 1243 cm^{-1} wavelengths are caused by C–C stretching and C–H bending bands. The Raman peak seen at a wavelength of 854 cm^{-1} characterizes the energy band gaps of the aromatic chains of the molecule. Raman peak with 756 cm^{-1} wavelength is based on C–C bending vibration bands. The main peaks of the PAA material are Raman spectra with wavelengths of 488, 645, 845, 1108, 1423, 1435, 1612, 1659, 2924, 3200 and 3330 cm^{-1}, respectively. Raman peak at 488 cm^{-1} wavelength is seen as C–C and C–H weak asymmetric bending vibrations caused by skeletal vibrations. The 645 cm^{-1} wavelength Raman peak is caused by the –CH and –CH$_2$ induced deformation vibration bands in the aromatic chain. The Raman peak seen at a wavelength of 845 cm^{-1} characterizes the energy band gaps of the aromatic chains of the molecule. Raman peak with 1108 cm^{-1} wavelength seen in the wavelength range of 1060–1127 cm^{-1} belongs to C–C symmetrical bending vibration bands. Raman peaks with 1423 and 1435 cm^{-1} wavelengths seen in the 1410–1460 cm^{-1} wavelength range are seen as deformation vibrations based on –CH$_2$ and –CH$_3$ functional groups. Raman peaks with wavelengths of 1612 cm^{-1} and 1659 cm^{-1} define mixed C=O vibrational stress bands with NH deformations. The Raman peak obtained at a wavelength of 2924 cm^{-1} is caused by –CH$_2$ asymmetric vibrational tension bands. Raman peaks seen at wavelengths of 3200 and 3330 cm^{-1} are characteristic for –NH shifted and expanded by hydrogen bonding (Dong et al. 1997).

XRD results

XRD (X-ray diffraction) was taken for dithizone and PAA materials. The final product with amorphous structure is shown in Fig. 1c spectrum taken for the PAA material. The diffraction peaks obtained for dithizone were 7.89°; 10.84°; 14.88°; 17.51°; 19.08°; 21.23°; 22.86°;23.89°; 25.20°;26.80°; 27.67°; 30.08° and 32.04°. XRD diffraction peaks are characteristic for dithizone material (Raharjo et al. 2008).

SEM results

SEM images (see Fig. 1d) of dithizone (a), PAA (b), and dithizone@PAA (c) materials were visualized by scanning electron microscopy. When the surface morphology of the
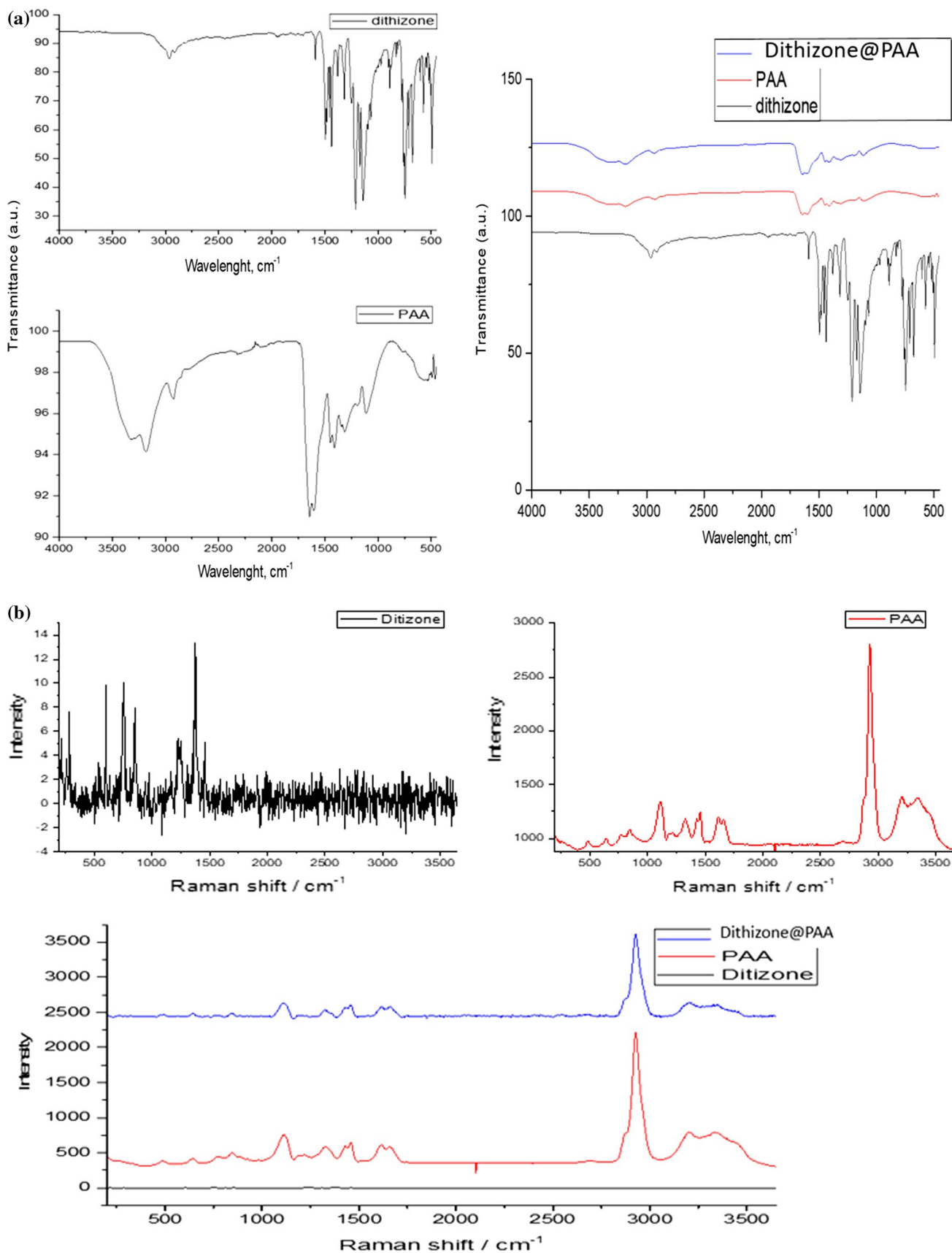
(a)

(b)

Fig. 1 **a** FTIR spectrums of developed material, **b** Raman spectrums of developed material, **c** XRD results of developed material, and **d** SEM images of developed material (a) Dithizone, (b) PAA (c) Dithizone@PAA
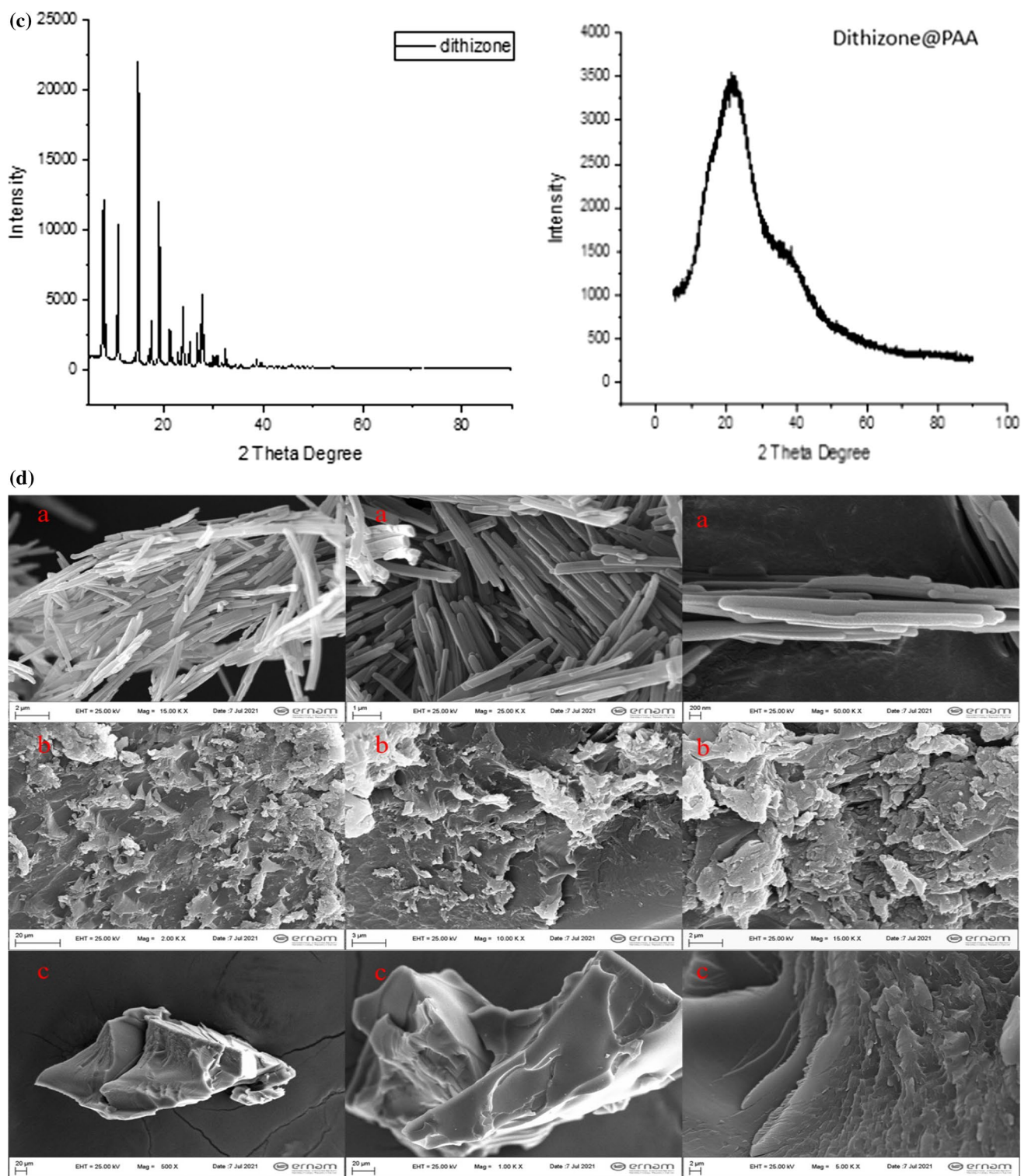
(c)

(d)

Fig. 1 (continued)

dithizone material is examined, it is seen that it has a rod (Rod) structure. Dithizone material, which is known to be easily soluble in organic solvents, lost its rod structure after its synthesis with PAA and was completely homogeneously dispersed in the polymer. As understood in the EDX analyses taken, the homogeneous distribution of the species in the dithizone structure was also proven in the synthesis product.

Optimization studies

For the optimization of the adsorption step, pH, shaking time and the amount of adsorbent were investigated step by step. For the optimization of the desorption step, the type and amount of eluent solvent and the vortex time were investigated. The percentage recovery of Mn(II) and Cu(II) ions was taken as reference in determining the optimum values of the relevant parameters. Recovery (%) is calculated according to the following formula.

$$\text{Recovery (\%)} = \left[C_{\text{found}} - C_{\text{real}} \right] \times 100 / C_{\text{spiked}} \tag{1}$$

where C_{found}, C_{real}, and C_{spiked} were the amount of the Mn(II) and Cu(II) after spiking the standard to the sample, amount of the sample, and amount of the standard solution that was injected to the sample, respectively.

Optimization of adsorption conditions

In order to obtain quantitative phase separation and acceptable analytical data, analyte ions must be effectively adsorbed on the adsorbent. Dithizone molecules is well known with a potential on making stable complexes with Mn and Cu ions. Complex formation reactions are affected with pH of medium (Kamnoet et al. 2021). To achieve this goal, the first factor to be optimized is the pH of the sample solution. Both adsorbent and analyte ions can exist in different forms depending on the pH value. This can increase or decrease the adsorption. To evaluate this effect, the effect of pH on the recovery of Mn(II) and Cu(II) ions was tested in the pH range of 3–8.5. It can be seen from Fig. 2a that recovery begins to decrease especially after pH 5.0 for both analytes. Phase separation was not effective, especially in the transition to the basic zone. Also, it is well known that hydroxy salts of these ions are observed beyond pH 7.0. So, acidic regions were scanned by using a buffer serie. A quantitative recovery was provided for analyte ions at pH 4.0. Therefore, pH 4.0 was chosen as optimum for the subsequent experimental studies.

The second factor optimized in the present study is the amount of adsorbent. In solid phase adsorbent studies, effective separation and preconcentration of analyte ions in sample solution directly depend on the amount of adsorbent. If the amount of adsorbent in the sample solution is insufficient, full adsorption of target ions cannot be achieved, as a result, quantitative phase separation and good analytical data cannot be obtained. So, the effect of the amount of adsorbent on the recovery of analyte ions was investigated in the range of 5–115 mg. The obtained data are given in Fig. 2b. At adsorbent amounts lower than 55 mg, quantitative analytical results could not be obtained due to insufficient phase separation. The amounts higher than 75 mg of adsorbent,

the partial reduction in recovery may be due to the increased volume of eluent required for the desorption of analyte ions. Therefore, 55 mg of adsorbent amount was chosen as optimum for the subsequent experimental studies. In order to accelerate the adsorption of analyte ions in the sample solution, the solutions were shaken at a certain constant speed using an orbital rotator. Also, thanks to this agitation step, the adsorbent was distributed evenly in the sample. In this context, the effect of adsorption time on recovery of analyte ions was investigated in the range of 1–40 min (see Fig. 2c). The results show that 20 min shaking time is sufficient for effective adsorption of analyte ions. Recovery of both analytes followed a flat plateau at periods greater than 20 min. Therefore, 20 min of adsorption time was chosen as optimum for the subsequent experimental studies.

Optimization of desorption conditions

A desorption study is required for the adsorbent containing the analytes separated from the aqueous solution after centrifugation. Here, the first factor to be investigated in order to effectively separate adsorbed analyte ions from the solid adsorbent into solution is the eluent solvent type. In this context, the effect of equal volumes of solvents such as water, pH 4.0 buffer, ethanol, methanol, THF and acidic ethanol on the recovery of analyte ions was investigated. The data obtained are given in Fig. 2d. When the results were examined, it was important to obtain non-quantitative recoveries, especially for water and pH 4.0 buffer solution. Because these solvents are used in adsorption–desorption studies. The best recovery for both analyte ions was observed in acidic EtOH. Therefore, acidic EtOH was chosen as eluent solvent for the subsequent experimental studies. The second variable optimized in the desorption step is the eluent (Ethanol) volume. The added eluent solvent must be sufficient to achieve the desorption of analyte ions. If large amount of eluent solvent is added, this will decrease the analyte concentration in the final volume and also increase the deformation of the adsorbent due to excessive eluent usage. For these reasons, the effect of acidic ethanol on the recovery of analyte ions was investigated in the range of 0.5–3.5 mL and the results obtained are exhibited in Fig. 2e. As seen from the results, complete desorption was achieved by the addition of 2.0 mL acidic ethanol for both analytes. The reduction in recovery at higher volumes are explained above. Therefore, 2.0 mL of acidic ethanol was chosen as optimum for the subsequent experimental studies. The last optimized factor for this step is desorption time. The effect of the desorption time on the recovery of analyte ions was investigated in the range of 20–180 s keeping other conditions constant. Figure 2f shows that 80 s as vortexing time is sufficient to complete desorption for both analytes. Since there is no significant change
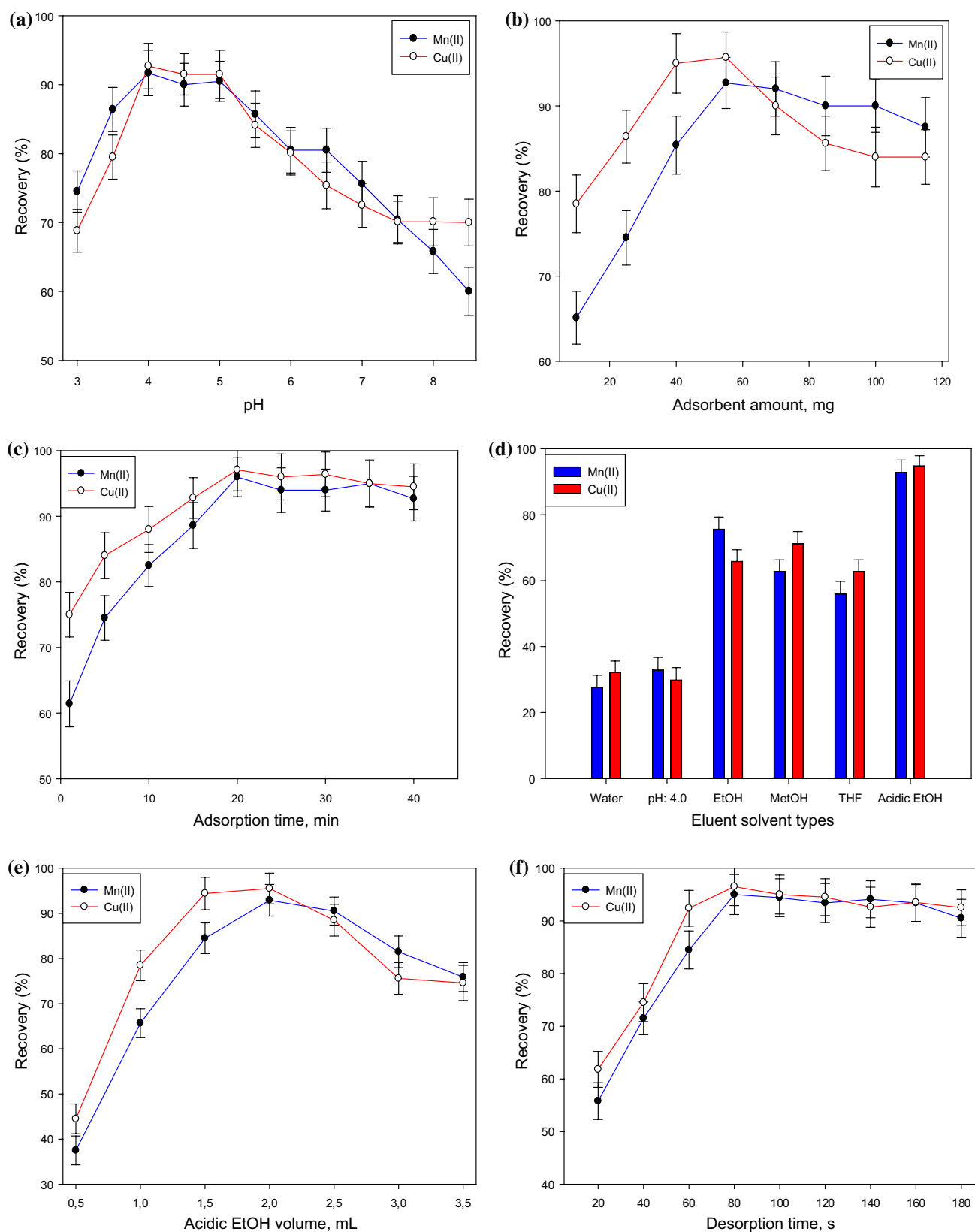
Fig. 2 Effect of **a** sample pH, **b** adsorbent amount, **c** adsorption time, **d** type of eluent solvent, **e** volume of desorption solvent, **f** desorption time on the recovery of Mn(II) and Cu(II). Microextraction conditions: sample volume, 100 mL; concentration of analytes, 50 µg L^{-1}; sample pH, 6.0; adsorbent amount, 55 mg, adsorption time, 20 min; desorption solvent, acidic EtOH; acidic EtOH volume, 2.0 mL; desorption time, 80 s

in the recovery of analyte ions at high vortex times, 80 s was chosen as the optimum value for next studies.

Adsorption capacity

Adsorption capacity is one of the important factors to evaluate the extraction efficiency of Mn(II) and Cu(II) ions. The adsorption capacity of the synthesized adsorbent for each analyte was determined according to the batch adsorption method. The related study includes the following experimental steps. 50 mL of model solution containing 20 mg of Mn(II) and Cu(II) ions was added to 100 mL beaker containing 55 mg of the adsorbent. Subsequently, the mixture was vortexed for about 1 h. After separation of the adsorbent from the aqueous solution, the possible amounts of analyte in the remaining aqueous portion were determined by FAAS using the formula in the batch adsorption method (Duran et al. 2011). As a result of this study, the adsorption capacity was calculated as 116.1 mg g^{-1} for Mn(II) and 132.8 mg g^{-1} for Cu(II), respectively.

Reusability

The high number of reusability of the synthesized adsorbent reduces the cost of the method. In this context, in order to test its reusability, the synthesized adsorbent was washed five times with ethanol and water after the desorption step and then dried for reuse. No significant change in recovery of Mn(II) and Cu(II) ions was observed until fifteen repetitions of the reuse of the adsorbent. The recoveries obtained were in the range of 97.3–99.2% for Mn(II) and 96.1–98.9% for Cu(II). The analytical data showed that the adsorbent was stable in the SA-DSPME procedure and had excellent reusability. The high number of reusability of the adsorbent caused a relative decrease in the cost of the method.

Analytical evaluations

Figures of merit of method

Under the optimized conditions, regression equations for the Mn(II) and Cu(II) ions were $A = 0.0393C_{Mn} + 0.0186$ and $A = 0.0461C_{Cu} - 0.0052$ with the correlation coefficient (r) of 0.9986 and 0.9992, respectively. Linear dynamic ranges for Mn(II) and Cu(II) were 0.7–150 ng mL^{-1} and 0.2–125 ng mL^{-1} with the detection limit (LOD) of 0.2 and 0.06 ng mL^{-1}, respectively. The relative standard deviations (RSD%, N:5) of 3.1 and 2.5% were obtained at 75 ng mL^{-1} level of Mn(II) and Cu(II) ions, respectively. The preconcentration factor (PF), defined as the ratio of the maximum volume of the starting solution (100 mL) to the final measuring volume of the extract (2 mL), was 50 for both analytes. Enhancement factor (EF), defined as the ratio of the slope of calibration plots with and without the SA-DSPME, was calculated as 136 and 175 for Mn(II) and Cu(II), respectively. Comprehensive analytical data are given in Table 1.

Selectivity

The selectivity of the synthesized adsorbent for Mn(II) and Cu(II) ions was tested by adding different amounts of anions and cations to model solutions containing analytes. The present study was performed in real samples, often in the presence of ions accompanying the investigated analyte ions. The tolerable concentration for ions refers to the maximum amount that causes an error not greater than ±5% in absorbance of the Mn(II) and Cu(II) ions. The results in Table 2 show that the recovery of Mn(II) and Cu(II) ions by the synthesized adsorbent does not change significantly, even at high matrix ion concentrations. Therefore, the investigated ions do not interfere with the SA-DSPME procedure and the synthesized adsorbent has high selectivity toward Mn(II) and Cu(II) ions. And also, it should be kept in mind that

Table 1 Related analytical parameters of the SA-DSPME-FAAS method for determination of Mn and Cu

Analytical parameters	Mn(II)	Cu(II)
Regression equation	$A = 0.0393C_{Mn} + 0.0186$	$A = 0.0461C_{Cu} - 0.0052$
Correlation coefficient (r)	0.9986	0.9992
Linear dynamic range (ng mL^{-1})	0.7–150	0.2–125
Limit of detection (LOD, ng mL^{-1})	0.2	0.06
Limit of quantitation (LOQ, ng mL^{-1})	0.7	0.2
Recovery (%) (75 ng mL^{-1}, N:5)	98.2	97.9
RSD (%) (75 ng mL^{-1}, N:5)	3.1	2.5
Preconcentration factor	50	50
Enhancement factor	136	175
Adsorption capacity (mg g^{-1})	116.1	132.8

LOD and LOQ were defined as $3S_b/m$ and $10S_b/m$, respectively (where S_b and m were the standard deviations of the sample blank and the slope of the calibration curves, respectively)

Table 2 The effect of interfering ions on recovery of 100 ng mL^{-1} of Mn(II) and 75 ng mL^{-1} Cu(II) ($N = 3$)

Ion	Added as	Tolerable concentration	Recovery (Mean ± standard deviations)	
			Mn (II)	Cu (II)
Na$^+$	NaNO$_3$	5000	97.3 ± 2.4	98.1 ± 2.6
K$^+$	KCl	5000	96.5 ± 3.6	97.6 ± 2.0
SO$_4^{2-}$	Na$_2$SO$_4$	5000	98.9 ± 4.1	97.3 ± 3.1
PO$_4^{3-}$	Na$_3$PO$_4$	2000	102.5 ± 3.0	98.5 ± 2.2
Mg^{2+}	Mg (NO$_3$)$_2$	2000	101.7 ± 3.8	95.8 ± 1.9
Ca^{2+}	Ca(NO$_3$)$_2$·4H$_2$O	2000	97.3 ± 1.9	103.5 ± 2.2
NO$_3^-$	Ni(NO$_3$)$_2$	2000	101.9 ± 2.4	97.0 ± 1.5
Al^{3+}	Al(NO$_3$)$_3$·9H$_2$O	1000	98.6 ± 2.9	99.4 ± 4.3
Ag$^+$	AgNO$_3$	1000	98.4 ± 3.5	98.8 ± 3.8
CH$_3$COO$^-$	CH$_3$COONa	1000	97.5 ± 3.7	98.2 ± 4.1
Fe^{3+}	FeCl$_3$·6H$_2$O	500	97.3 ± 4.8	97.6 ± 2.6
Co^{2+}	Co(NO$_3$)$_2$·6H$_2$O	500	98.2 ± 1.9	98.8 ± 3.4
Ni^{2+}	Ni(NO$_3$)$_2$·6H$_2$O	500	103.5 ± 3.6	95.4 ± 2.5
Pb^{2+}	Pb(NO$_3$)$_2$	250	100.7 ± 2.3	96.2 ± 3.7
Cr^{2+}	Cr(NO$_3$)$_2$	250	95.9 ± 2.7	104.4 ± 2.8
Zn^{2+}	Zn(NO$_3$)$_2$·6H$_2$O	100	95.5 ± 3.5	102.3 ± 3.6

the selectivity provided by hallow cathode lamb (HCL) in FAAS. As well known, even trace amounts of some foreign ions were attached on solid phase material, interferences of these ions will not be observed in determination step thanks to selectivity of HCL for target ions.

Precision

The intraday precision was evaluated in model solutions at the three concentration levels of Mn(II) (10, 50 and 150 ng mL^{-1}) and Cu(II) (1, 10 and 50 ng mL^{-1}) ions, by performing five replicates daily. The same concentrations were analyzed five times each day, for a period of five days, for the inter-day precision. The intraday and inter-day precision for Mn(II) ions were in the range from 3.8 to 5.3% and from 4.3 to 5.6%, respectively, while the intraday and inter-day precision for Cu (II) ions were in the range of 3.2–5.4% and 3.6–5.7%, respectively. Also, satisfactory recoveries were provided for both studies. Detailed data are given in Table 3.

Accuracy

In order to investigate the accuracy of the developed SA-DSPME procedure, the experiments were applied for the determination of Mn and Cu in reference materials such as SRM-1568 Rice Flour, INCT-TL-1 Tea leaves, INCT-MPH-2 Mixed Polish Herbs and SRM-1515 apple leaves. As can be seen from Table 4, the data obtained agreed well with the reference results. Analyzing the four reference materials, the recoveries ranged from 95.9 to 100.9%. In addition, the t-values obtained for CRMs were in the range 0.81–1.62, and these values were considerably lower than the tabulated t-value (2.78) at the 95% confidence level for five measurements. These results confirmed the accuracy of the developed method.

Real sample analysis

Following the validation studies, the applicability of the developed SA-DSPME-FAAS method was investigated by analysis of manganese and copper ions in fortified vegetables (sesame, groundnut, eggplant, corn, and cucumber) and barbecue samples (grilled fish, grilled chicken, meat doner, meatball, and chicken doner). The samples prepared according to the microwave digestion method described above were analyzed three times. In addition, the accuracy of the obtained data was investigated through a recovery study by adding the samples at two levels of Mn(II) and Cu(II) ions. The analytical data and the respective standard deviations are given in Table 5. The results obtained showed that the matrices of the samples do not have a significant effect on the performance of the developed method. Recovery (%) for Mn (II) and Cu (II) was obtained in the range of 94% to 104% and 92 to 105%, respectively, indicating the good applicability of the developed method for measuring Mn and Cu in the analyzed samples.

Comparison of the proposed study with published methods

Table 6 submits the figures of merits for the determination of Mn(II) and Cu(II) by the developed SA-DSPME-FAAS method with those of the previously reported analytical methods based on solid-phase microextraction. The EF value

Table 3 Intraday and inter-day precision for the SA-DSPME-FAAS method for determination of Mn and Cu

Mn(II)				Cu(II)			
Spiked (ng mL^{-1})	Recovery (%)	Inter-day	Intraday	Spiked (ng mL^{-1})	Recovery (%)	Inter-day	Intraday
10	94.2	3.8	4.3	1	93.1	3.2	3.6
50	97.2	4.2	5.0	10	96.2	4.0	4.9
100	98.5	5.3	5.6	50	97.9	5.5	5.7

Table 4 Determination of Mn and Cu in certified reference materials (N = 5)

Reference materials	Validation parameters	Experimental data	
		Mn	Cu
SRM 1568 (Rice Flour)	Certified value (mg kg^{-1})	19.2 ± 1.8	2.35 ± 0.16
	Found value (mg kg^{-1})	18.8 ± 0.9	2.31 ± 0.11
	Recovery (%)	97.9	98.3
	*t_{exp}	0.99	0.81
INCT-TL-1 (Tea leaves)	Certified value (mg kg^{-1})	1570 ± 11	20.4 ± 1.5
	Found value (µg kg^{-1})	1526 ± 87	19.9 ± 0.9
	Recovery (%)	97.2	97.5
	*t_{exp}	1.13	1.24
INCT-MPH-2 (Mixed Polish Herbs)	Certified value (µg kg^{-1})	191 ± 12	7.77 ± 0.53
	Found value (µg kg^{-1})	184 ± 11	7.45 ± 0.44
	Recovery (%)	96.3	95.9
	*t_{exp}	1.42	1.62
SRM 1515 (apple leaves)	Certified value (µg kg^{-1})	2710 ± 120	5.69 ± 0.13
	Found value (µg kg^{-1})	2623 ± 181	5.74 ± 0.12
	Recovery (%)	96.8	100.9
	*t_{exp}	1.07	0.93

*The tabulated *t*-value (2.78) at the 95% confidence level for five measurements

of the developed method was high and the linear range was relatively wide, except for ICP-OES and ICP-MS techniques. According to similar determination techniques, the LODs of the developed method were lower and RSDs% values were comparable. The developed method allowed acceptable analytical results with the use of inexpensive chemicals and instruments. These results show that the developed method has the advantage of low toxicity, reliability and efficiency.

Conclusion

In this research, a green and economic shake-assisted dispersive solid-phase microextraction coupled with flame atomic absorption spectrometry has been developed for simultaneous determination and preconcentration of manganese and copper in fortified vegetables and barbecue samples. New synthetized adsorbent for this study has been characterized by means of SEM, FTIR, XRD and Raman technical. Analytical data showed that the developed method can be used successfully for the analysis of Mn(II) and Cu(II) ions in the selected samples. Linear dynamic ranges for Mn(II) and Cu(II) were 0.7–150 ng mL^{-1} and 0.2–125 ng mL^{-1} with the LOD of 0.2 and 0.06 ng mL^{-1}, respectively. The proposed method has advantages, including simplicity, speed and low cost, in relation to classical sample preparation procedures. The method involved minimal manipulation of the sample,

Table 5 Analytical data obtained for Mn and Cu as a result of the application of the developed method to barbecue and fortified vegetable samples (N = 3)

Matrix	Mn (µg kg^{-1})			Cu (µg kg^{-1})		
	Added	Found	Recovery (%)	Added	Found	Recovery (%)
Sesame	–	74.5 ± 3.5	–	–	15.1 ± 0.8	–
	20	93.8 ± 4.8	97	50	62.6 ± 2.9	95
Groundnut	–	62.1 ± 2.6	–	–	32.8 ± 1.5	–
	20	81.5 ± 2.7	97	50	78.8 ± 3.1	92
Eggplant	–	95.7 ± 3.2	–	–	20.7 ± 1.4	–
	20	116.5 ± 4.4	103	50	73.2 ± 2.8	105
Corn	–	55.6 ± 1.9	–	–	6.4 ± 0.2	–
	20	74.4 ± 2.8	94	50	57.9 ± 2.1	103
Cucumber	–	88.9 ± 3.3	–	–	35.3 ± 1.8	–
	20	108.3 ± 4.6	97	50	83.3 ± 2.7	96
Grilled fish	–	124.5 ± 4.0	–	–	8.9 ± 0.3	–
	20	144.7 ± 5.3	101	50	59.9 ± 2.0	102
Grilled chicken	–	26.7 ± 2.1	–	–	nd	–
	20	47.1 ± 1.8	102	50	48.5 ± 1.9	97
Meat Doner	–	nd*	–	–	nd	–
	20	19.8 ± 1.1	99	50	51.5 ± 2.1	103
Meatball	–	144.2 ± 5.6	–	–	28.3 ± 1.4	–
	20	163.4 ± 6.2	96	50	75.3 ± 1.7	94
Chicken doner	–	65.8 ± 3.9	–	–	7.4 ± 0.2	–
	20	86.6 ± 4.0	104	50	56.4 ± 1.8	98

*Not dedection

Table 6 Comparative data from studies about preconcentration investigated metal ions adsorbent

Adsorbent	Analytical technique	LDR (ng mL^{-1})		LOD (ng mL^{-1})		PF or EF		RSD (%)		Reusability	Application	References
		Mn	Cu	Mn	Cu	Mn	Cu	Mn	Cu			
Graphene oxide/PTT	FAAS	20–3500	10–2600	0.49	0.06	280		1.3	1.8	4	Spinach, honey, hair, blood and waters	(Pourjavid et al. 2016)
C18-cartridge	ICP OES	–	–	0.5	0.02	10	13	3	2	11	Environmental waters	(Carvalho et al. 2015)
CoFe$_2$O$_4$ nanoparticles	EDXRF	27–400	36–400	9	12	25	25	4.5	1.6	5	Ethanol fuel samples	(Meira et al. 2018)
C.silvaticus immobilized MWCNT	ICP OES	–	0.7–28.6	–	0.014	–	60	–	1.1	30	Foods and waters	(Ozdemir et al. 2019)
Nanosized spongelike Mn$_3$O$_4$	FAAS	–	100–1000	–	2.6	–	20	–	3.2	100	Food and herb samples	(Yavuz et al. 2016)
Poly(styrene)-co-2-vinylpyridine	FAAS	0.1–300	–	0.03	–	115	–	7.6	–	12	Foods and vegetables	(Tüzen et al. 2020)
Oxidized multiwalled carbon nanotubes	ICP-OES	0.5–1000	–	0.12	–	50	–	2.4	–	–	Foods	(Feist et al. 2019)
Graphene oxide–silica composite	ICP-MS	0.03–50	0.1–50	0.0075	0.002	10	10	7.2	7.3	5	Environmental samples	(Su et al. 2014)
Dithizone@PAA	FAAS	0.7–150	0.2–125	0.2	0.06	136	175	3.1	2.5	15	Vegetables and barbecue samples	Current method

FAAS flame atomic absorption spectrometry; *ICP OES* inductively coupled plasma optical emission spectrometry; *EDXRF* energy-dispersive X-ray fluorescence spectrometry; *ICP-MS* inductively coupled plasma mass spectrometry

favoring the reduction in contamination, in addition, as it does not require conventional heating in the preparation step, the losses of analytes by volatilization are reduced. The analytical properties of the developed method are suitable for routine analysis laboratories which don't have expensive instrumental equipment's.

Declarations

Conflict of interest The authors have declared that there is no conflict of interest.

References

Acikkapi AN, Tuzen M, Hazer B (2019) A newly synthesized graft copolymer for magnetic solid phase microextraction of total selenium and its electrothermal atomic absorption spectrometric determination in food and water samples. Food Chem 284:1–7

Adhikary P, Tiwari KN, Singh RP (2007) Synthesis, characterization, and flocculation characteristics of polyacrylamide-grafted glycogen. J Appl Polym Sci 103(2):773–778

Ali J, Tuzen M, Feng X, Kazi TG (2021) Determination of trace levels of selenium in natural water, agriculture soil and food samples by vortex assisted liquid-liquid microextraction method: multivariate techniques. Food Chem 344:128706

Altunay N, Elik A, Bulutlu C, Gürkan R (2018) Application of simple, fast and eco-friendly ultrasound-assisted-cloud point extraction for pre-concentration of zinc, nickel and cobalt from foods and vegetables prior to their flame atomic absorption spectrometric determinations. Int J Environ Anal Chem 98(7):655–675

Altunay N, Katin KP (2020) Ultrasonic-assisted supramolecular solvent liquid-liquid microextraction for determination of manganese and zinc at trace levels in vegetables: experimental and theoretical studies. J Mol Liq 310:113192

Arain SA, Kazi TG, Afridi HI, Arain MS, Panhwar AH, Khan N, Shah F (2016) A new dispersive liquid–liquid microextraction using ionic liquid based microemulsion coupled with cloud point extraction for determination of copper in serum and water samples. Ecotoxicol Environ Saf 126:186–192

Carvalho FP (2017) Pesticides, environment, and food safety. Food Energy Secur 6(2):48–60

Carvalho RN, Brito GB, Korn MG, Teixeira JS, Dias FDS, Dantas AF, Teixeira LS (2015) Multi-element determination of copper, iron, nickel, manganese, lead and zinc in environmental water samples by ICP OES after solid phase extraction with a C18 cartridge loaded with 1-(2-pyridylazo)-2-naphthol. Anal Methods 7(20):8714–8719

Chiem LT, Huynh L, Ralston J, Beattie DA (2006) An in situ ATR–FTIR study of polyacrylamide adsorption at the talc surface. J Colloid Interface Sci 297(1):54–61

Diduch SL, Losev VN, Mukhina AN, Trofimchuk AK (2016) Using silica modified by tiron for metal preconcentration and determination

in natural waters by inductively coupled plasma atomic emission spectrometry. J Anal Chem 71(11):1081–1088

Dong J, Ozaki Y, Nakashima K (1997) Infrared, Raman, and near-infrared spectroscopic evidence for the coexistence of various hydrogen-bond forms in poly (acrylic acid). Macromolecules 30(4):1111–1117

Duran C, Ozdes D, Gundogdu A, Imamoglu M, Senturk HB (2011) Tea-industry waste activated carbon, as a novel adsorbent, for separation, preconcentration and speciation of chromium. Anal Chim Acta 688(1):75–83

Elik A, Altunay N, Gürkan R (2017) Microextraction and preconcentration of Mn and Cd from vegetables, grains and nuts prior to their determination by flame atomic absorption spectrometry using room temperature ionic liquid. J Mol Liq 247:262–268

Feist B, Sitko R (2019) Fast and sensitive determination of heavy metal ions as batophenanthroline chelates in food and water samples after dispersive micro-solid phase extraction using graphene oxide as sorbent. Microchem J 47:30–36

Godwin-Uranta K, Rezaei-Gomari S, Russell P, Hamad F (2018) Studying the effectiveness of polyacrylamide (PAM) application in hydrocarbon reservoirs at different operational conditions. Energies 11(9):2201

Gouda AA, AlShehri AM, El Sheikh R, Hassan WS, Ibrahim SH (2020) Development of green vortex-assisted supramolecular solvent-based liquid–liquid microextraction for preconcentration of mercury in environmental and biological samples prior to spectrophotometric determination. Microchem J 157:105108

Kamnoet P, Aeungmaitrepirom W, Menger RF, Henry CS (2021) Highly selective simultaneous determination of Cu (II), Co (II), Ni (II), Hg (II), and Mn (II) in water samples using microfluidic paper-based analytical devices. Analyst 146(7):2229–2239

Li YO, Komarek AR (2017) Dietary fibre basics: health, nutrition, analysis, and applications. Food Qual Saf 1(1):47–59

Manjusha R, Shekhar R, Kumar SJ (2019) Ultrasound-assisted extraction of Pb, Cd, Cr, Mn, Fe, Cu, Zn from edible oils with tetramethylammonium hydroxide and EDTA followed by determination using graphite furnace atomic absorption spectrometer. Food Chem 294:384–389

Meira LA, Almeida JS, Dias FDS, Pedra PP, Pereira ALC, Teixeira LS (2018) Multi-element determination of Cd, Pb, Cu, V, Cr, and Mn in ethanol fuel samples using energy dispersive X-ray fluorescence spectrometry after magnetic solid phase microextraction using CoFe2O4 nanoparticles. Microchem J 142:144–151

Menghwar P, Yilmaz E, Sherazi STH, Soylak M (2019) A sensitive and selective deep eutectic solvent-based ultrasound-assisted liquid phase microextraction procedure for separate ion-preconcentration and determination of copper in olive oil and water samples. Sep Sci Technol 54(15):2431–2439

Nimse SB, Pal D (2015) Free radicals, natural antioxidants, and their reaction mechanisms. RSC Adv 5(35):27986–28006

Ogunkunle ATJ, Bello OS, Ojofeitimi OS (2014) Determination of heavy metal contamination of street-vended fruits and vegetables in Lagos state, Nigeria. Int Food Res J 2014:21(5)

Oymak T, Ulusoy Hİ, Hastaoglu E, Yılmaz V, Yıldırım Ş (2017) Some heavy metal contents of various slaughtered cattle tissues in Sivas-Turkey. J Turk Chem Soc Sect A: Chem 4(3):721–728

Ozdemir S, Kilinc E, Oner ET (2019) Preconcentrations and determinations of copper, nickel and lead in baby food samples employing Coprinus silvaticus immobilized multi-walled carbon nanotube as solid phase sorbent. Food Chem 276:174–179

Peng G, He Q, Zhou G, Li Y, Su X, Liu M, Fan L (2015) Determination of heavy metals in water samples using dual-cloud point extraction coupled with inductively coupled plasma mass spectrometry. Anal Methods 7(16):6732–6739

Pourjavid MR, Arabieh M, Yousefi SR, Sehat AA (2016) Interference free and fast determination of manganese (II), iron (III) and copper (II) ions in different real samples by flame atomic absorption spectroscopy after column graphene oxide-based solid phase extraction. Microchem J 129:259–267

Pytlakowska K, Matussek M, Hachuła B, Pilch M, Kornaus K, Zubko M, Pisarski WA (2018) Graphene oxide covalently modified with 2, 2′-iminodiacetic acid for preconcentration of Cr (III), Cu (II), Zn (II) and Pb (II) from water samples prior to their determination by energy dispersive X-ray fluorescence spectrometry. Spectrochim Acta, Part B 147:79–86

Raharjo G, Tahir I, Wahyuni ET (2008) Immobilization of Dithizone onto chitin isolated from prawn seawater shells (P. merguensis) and its preliminary study for the adsorption of Cd (II) ion 1:1–7

Rapp I, Schlosser C, Rusiecka D, Gledhill M, Achterberg EP (2017) Automated preconcentration of Fe, Zn, Cu, Ni, Cd, Pb Co, and Mn in seawater with analysis using high-resolution sector field inductively-coupled plasma mass spectrometry. Anal Chim Acta 976:1–13

Saadati S, Eduok U, Abdelrasoul A, Shoker A (2020) A surface-enhanced Raman scattering-based approach for rapid and highly sensitive quantitative analysis of 3-carboxy-4-methyl-5-propyl-2-furanpropionate and indole-3-acetic acid in saline, human serum and uremic serum of patients with chronic kidney disease. RSC Adv 10(71):43489–43496

Shirkhanloo H, Khaligh A, Mousavi HZ, Rashidi A (2016) Ultrasound assisted-dispersive-micro-solid phase extraction based on bulky amino bimodal mesoporous silica nanoparticles for speciation of trace manganese (II)/(VII) ions in water samples. Microchem J 124:637–645

Şimşek S, Şenol ZM, Ulusoy Hİ (2017) Synthesis and characterization of a composite polymeric material including chelating agent for adsorption of uranyl ions. J Hazard Mater 338:437–446

Şimşek S, Ulusoy Hİ (2016) Effective mercury removal using a new developed polymer containing 2-(2'thiazolylazo) p-cresol. Environ Eng Manag J 15(11)

Su S, Chen B, He M, Hu B (2014) Graphene oxide–silica composite coating hollow fiber solid phase microextraction online coupled with inductively coupled plasma mass spectrometry for the determination of trace heavy metals in environmental water samples. Talanta 123:1–9

Tokman N (2007) The use of slurry sampling for the determination of manganese and copper in various samples by electrothermal atomic absorption spectrometry. J Hazard Mater 143:87–94

Tuzen M, Elik A, Hazer B, Şimşek S, Altunay N (2020) Poly (styrene)-co-2-vinylpyridine copolymer as a novel solid-phase adsorbent for determination of manganese and zinc in foods and vegetables by FAAS. Food Chem 333:127504

Ulusoy Hİ (2017) A versatile hydrogel including bentonite and gallocyanine for trace Rhodamine B analysis. Colloids Surf A 513:110–116

Vassileva E, Wysocka I, Orani AM, Quétel C (2019) Off-line preconcentration and inductively coupled plasma sector field mass spectrometry simultaneous determination of Cd Co, Cu, Mn, Ni, Pb and Zn mass fractions in seawater: procedure validation. Spectrochim Acta Part B 153:19–27

Walker RE, Keane CR, Burke JG (2010) Disparities and access to healthy food in the United States: a review of food deserts literature. Health Place 16(5):876–884

Yavuz E, Tokalıoğlu Ş, Şahan H, Patat Ş (2016) Nanosized spongelike Mn3O4 as an adsorbent for preconcentration by vortex assisted solid phase extraction of copper and lead in various food and herb samples. Food Chem 194:463–469